Advances in Water Resources 32 (2009) 1206–1212

Contents lists available at ScienceDirect

Advances in Water Resources

journal homepage: www.elsevier.com/locate/advwatres

Steady state heat transport in 3D heterogeneous porous media

Juan J. Hidalgo [a,*], Jesús Carrera [b], Marco Dentz [a,b]

[a] Department of Geotechnical Engineering and Geosciences, Technical University of Catalonia (UPC), Jordi Girona 1-3, Mod. D2-004, 08034 Barcelona, Spain
[b] Institute of Environmental Assessment and Water Research (IDAEA), CSIC, Lluís Solé i Sabarís s/n, 08028 Barcelona, Spain

ARTICLE INFO

Article history:
Received 20 December 2008
Received in revised form 6 April 2009
Accepted 16 April 2009
Available online 7 May 2009

Keywords:
Heat transport
Aquifer thermal energy storage
Dispersion
Heterogeneity
Groundwater

ABSTRACT

Heat is transported in aquifers by advection and conduction. Spatial variability of hydraulic conductivity causes fluctuations in small scale advection, whose effect can be represented by a dispersion term. However, the use of this term is still subject to controversy among modelers. The effect of heterogeneity on the heat plume generated by a groundwater heat exchanger (GHE) in a three-dimensional aquifer under steady state conditions is examined. Transverse dispersion is estimated using a stochastic approach in which a distinction between effective and ensemble dispersion coefficients is made. The former quantifies the typical width of the heat plume and the latter takes into account the uncertainty of the lateral plume position. Simulations show that transverse dispersion is proportional to the variance and correlation length of the log-conductivity field. On the one hand, the ensemble transverse dispersion coefficient, which can be used for risk analysis to find the mean temperature and the potential plume spread, is high near the heat source and then decreases. On the other hand, the effective transverse dispersion coefficient, the one required to simulate actual temperature values and plume width, displays a less marked dependence on the distance from the source. For modeling purposes it can be approximated as $\alpha_T \approx 0.02\sigma^2_{\ln K} L_x$, where $\sigma^2_{\ln K}$ is the variance of the log-conductivity field and L_x its correlation length in the mean flow direction. However, a zero dispersion should be used to compute the energy dissipated by the GHE.

1. Introduction

The use of groundwater for energy storage and heat exchange has been an issue of great interest since the 1970s. Aquifers are considered a source of clean, environment friendly energy and are increasingly used to reduce the need for other energy sources [1–3]. However, the thermal use of aquifers alters the natural temperature distribution of groundwater, which can affect groundwater quality. Changes in temperature can also interfere with other aquifers usages, surface water systems or influence the performance of thermal devices. Understanding groundwater heat transport is essential for the design, performance analysis and impact assessment of thermal devices. Understanding is often gained through numerical modeling, which allows synthesizing and integrating the knowledge obtained from field observations.

Heat transport is frequently modeled subject to approximations that help in solving the problem without losing the relevant aspects of the phenomenon. Heat transport models often disregard density and viscosity changes caused by temperature (e.g. [4,5,3]). Thermal properties of the soil (conductivity and heat capacity) are usually considered homogeneous or only dependent on the geological facies (e.g. [6–8]). It is also frequent to disregard heterogeneity in hydraulic conductivity. Finally, hydrodynamic dispersion is sometimes considered negligible compared to other transport mechanisms, i.e., conduction and advection. While the impact and applicability limits of the approximations on water and soil properties are well established [9], the effect of heterogeneity and dispersion on heat transport is still subject to some debate.

The relationship between dispersion and heterogeneity has been intensively studied for solute transport (e.g. [10,11]). Solute and energy transport obey very similar equations. Therefore, similar behavior should be expected. However, heat diffusion is several orders of magnitude higher than molecular diffusion (10^{-4}–10^{-5} m^2/s for heat diffusivity against 10^{-9}–10^{-10} m^2/s for molecular diffusion), which may have a smoothing effect on the temperature contrast caused by spatial heterogeneity. Recently, Ferguson [12] studied the effect of heterogeneity on the injection and later pumping of warm water in an aquifer. He found that heterogeneity decreases the amount of energy recovered and increases the uncertainty in temperature distribution.

Traditionally, heat dispersion has been considered a process of a lower order than conduction [13–15] or convection [16]. When acknowledged, dispersion is treated in diverse manners. Woodbury and Smith [4] provide a criteria based on the Peclet number to determine if the regime is conduction dominated. Doughty et al.

* Corresponding author. Tel.: +34 934017244; fax: +34 934017251.
E-mail addresses: juan.hidalgo@upc.edu (J.J. Hidalgo), jcarrera@ija.csic.es (J. Carrera), marco.dentz@upc.edu (M. Dentz).

0309-1708/$ - see front matter © 2009 Elsevier Ltd. All rights reserved.
doi:10.1016/j.advwatres.2009.04.003

[17] consider that an effective conductivity value independent of the velocity can be sufficient to represent dispersion in heat transport models. Sauty et al. [18] define an effective conductivity linear on velocity to simulate heat transport under radial flow conditions. However, Willemsen and Groeneveld [19] (quoted by Chevalier and Banton [20]) state that the addition of a dispersive term can overestimate the process.

In practice there is no agreement about the need for heat dispersion, as pointed out by Anderson [21] and Ferguson and Woodbury [2]. Some modelers include it (e.g. [13,22]) while others do not (e.g. [8,23]). In particular, the absence of heat dispersion is a common characteristic of groundwater heat exchangers (GHE) models (e.g. [7,24,3]), where only advection and conduction are considered.

The aim of this work is to study the importance of hydraulic conductivity heterogeneity on heat transport, so as to shed light on whether dispersion is needed or not. For this purpose, a steady state heat plume originating from a GHE will be modeled in a three-dimensional heterogeneous aquifer. The characterization of the plume will be studied using a stochastic framework. Special attention will be paid to the effect of heterogeneity on transverse dispersion and the energy mass balance.

2. Governing equations

Equations governing water flow and heat transport in aquifers are presented in this section. Flow is described by Darcy's law and local scale transport is characterized by advection and heat conduction. As a first approximation, density and viscosity changes will be considered negligible because the range of temperatures used is small. Under these assumptions, steady state flow and transport are described by the following governing equations:

$$\nabla \cdot [K(\mathbf{r})\nabla h(\mathbf{r})] = 0, \tag{1}$$

$$\mathbf{q}(\mathbf{r}) \cdot \nabla T(\mathbf{r}) - D\nabla^2 T(\mathbf{r}) = j_s'(\mathbf{r}), \tag{2}$$

with

$$D = \frac{\lambda}{\rho_w c_w} \quad \text{and} \quad j_s'(\mathbf{r}) = \frac{j_s(\mathbf{r})}{\rho_w c_w}, \tag{3}$$

where $\mathbf{r}$ [L] is the coordinate vector, K [L T^{-1}] is hydraulic conductivity, h [L] is piezometric head, T [K] is temperature, $\mathbf{q}$ [L T^{-1}] is Darcy flux,

$$\mathbf{q}(\mathbf{r}) = -K(\mathbf{r})\nabla h(\mathbf{r}), \tag{4}$$

ρ_w [M L^{-3}] is water density, c_w [L^2 T^{-2} K^{-1}] is the specific heat of water, λ [M L T^{-3} K^{-1}] is the medium thermal conductivity and j_s [M L T^{-3}] is a heat source.

The above steady state transport problem can be solved analytically for an infinite homogeneous aquifer with natural flow and transport boundary conditions. Without loss of generality, the flow field can be assumed to be aligned with the x-direction, i.e., $\mathbf{q} = q_0\hat{\mathbf{e}}_x$, where q_0 is the mean regional groundwater flux. For a point-like source in two dimensions (or line-like source along the z-direction in three dimensions) the temperature distribution is given by [25]

$$T(\mathbf{r}) = \frac{j_s'}{2\pi D}\exp\left(\frac{q_0 x}{2D}\right)K_0\left[\frac{q_0(x^2+y^2)}{2D}\right], \tag{5}$$

where K_0 is the modified Bessel function of the second kind of order zero.

3. Characterization of heat dispersion

The steady state heat plume in a homogeneous medium is shaped by advection in the direction of flow and by lateral dispersion (5). The longitudinal dispersion can be neglected as can be seen in (5), which describes an elongated plume with small gradients in the flow direction. In analogy, the plume shape in a heterogeneous medium can be described by the evolution of its lateral extension along the mean flow direction. The extension of a plume is typically measured by the spatial moments of the temperature distribution [26,27]. Therefore, the plume can be described by the evolution in the flow direction of the transverse second order spatial moment. The effect of heterogeneity can be systematically studied using a stochastic modeling framework in which observables are defined as suitable averages over the ensemble of all possible medium realizations. In summary, heat dispersion will be characterized here by the ensemble averages of the transverse moments of the temperature distribution. The basics of this methodology are presented next.

3.1. Transverse spatial moments

The zeroth, first and second transverse spatial moments of the steady state heat plume are defined as

$$\mu^{(0)}(x) = \int \mathrm{d}\mathbf{r}_T\, T(\mathbf{r}), \tag{6}$$

$$\mu_i^{(1)}(x) = \int \mathrm{d}\mathbf{r}_T\, r_i T(\mathbf{r}), \tag{7}$$

$$\mu_{ii}^{(2)}(x) = \int \mathrm{d}\mathbf{r}_T\, r_i^2 T(\mathbf{r}), \tag{8}$$

where $i = y, z$ and $\mathbf{r}_T = (y, z)^t$.

For a given cross-section of the medium, $\mu^{(0)}(x)$ is a measure for the stored energy and $\mu_i^{(1)}(x)$ is the transverse position of the plume center of mass. The lateral plume extent is quantified by the second centered moments of the normalized temperature distribution

$$\kappa_{ii}(x) = \frac{\mu_{ii}^{(2)}(x)}{\mu^{(0)}(x)} - \left[\frac{\mu_i^{(1)}(x)}{\mu^{(0)}(x)}\right]^2 \quad \text{for } i = y, z. \tag{9}$$

A relation between the above defined transverse moments and the dispersion of the heat plume can be obtained for the homogeneous case (i.e., $q_i = q_0\delta_{i1}$) for a line-like heat source (i.e., $j'(\mathbf{r}) = Q\delta(x,y)$, where Q [K T^{-1}] is constant). Disregarding longitudinal dispersion because $\partial T/\partial x \ll \partial T/\partial \mathbf{r}_T$, (2) reduces to

$$q_0\frac{\partial T(\mathbf{r})}{\partial x} - D\left(\frac{\partial^2 T(\mathbf{r})}{\partial y^2} + \frac{\partial^2 T(\mathbf{r})}{\partial z^2}\right) = Q\delta(x,y). \tag{10}$$

Multiplying Eq. (10) by y^2 and integrating it by parts in the transverse direction yields

$$q_0\frac{\partial \mu_{yy}^{(2)}(x)}{\partial x} - 2D = 0, \tag{11}$$

which is obtained taking into account that when $\mathbf{r} \to \infty$, T and ∇T vanish, and that the integral of the source term is null for symmetry. Integrating (11) and substituting $\mu_{yy}^{(2)}$ into (9) yields

$$\kappa_{yy}(x) = \frac{2D}{q_0}x. \tag{12}$$

Note that for the homogeneous case $\mu^{(0)}$ is constant and $\mu_y^{(1)}(x) = 0$.

Eq. (12) shows that the transverse width of the steady state plume increases as $\sqrt{x}$ and establishes a relation between the transverse moment and the dispersion coefficient. This relation can be generalized to the heterogeneous case to measure the rate of increase of the transverse plume extension along the x-direction. A transverse dispersion coefficient D_T can be defined as

$$D_T = \frac{1}{2}\frac{\mathrm{d}\kappa_{yy}(x)}{\mathrm{d}x}q_0, \tag{13}$$

where q_0 is the mean flow for the heterogeneous case.

3.2. Stochastic model and ensemble averages

In the stochastic approach, the spatially varying conductivity field $K(\mathbf{r})$ is modeled as a typical realization of an ensemble of conductivity fields $\{K(\mathbf{r})\}$, which is characterized by its joint distribution density $\mathscr{P}\{K(\mathbf{r})\}$. Hydraulic conductivity is found to be log-normally distributed, so that it can be completely characterized by the mean and semivariogram of the log-conductivity field $f(\mathbf{r}) = \ln K(\mathbf{r})$.

In a stochastic model, the definition of the plume width is not unique and depends on the order in which averages are taken. This has been extensively studied for the transport of contaminant plumes in heterogeneous porous media (e.g. [27–31]). In this spirit, an effective and ensemble plume widths can be defined. The effective plume width is defined by ensemble averaging over the second centered moments in single realizations

$$\kappa_{ii}^{\text{eff}}(x) = \langle \kappa_{ii}(x) \rangle \quad \text{for } i = y, z, \tag{14}$$

where the angular brackets denote the average over all realizations. The ensemble plume width is defined in terms of the second centered moment of the ensemble averaged heat distribution $\langle T(\mathbf{r}) \rangle$

$$\kappa_{ii}^{\text{ens}}(x) = \frac{\langle \mu_{ii}^{(2)}(x) \rangle}{\langle \mu^{(0)}(x) \rangle} - \left[\frac{\langle \mu_{i}^{(1)}(x) \rangle}{\langle \mu^{(0)}(x) \rangle} \right]^2 \quad \text{for } i = y, z. \tag{15}$$

Accordingly, the effective and ensemble transverse dispersion coefficients are defined by

$$D_T^{\text{ens}} = \frac{1}{2} \frac{\mathrm{d}\kappa_{yy}^{\text{ens}}(x)}{\mathrm{d}x} q_0 \tag{16}$$

and

$$D_T^{\text{eff}} = \frac{1}{2} \frac{\mathrm{d}\kappa_{yy}^{\text{eff}}(x)}{\mathrm{d}x} q_0, \tag{17}$$

respectively.

The effective quantities measure the evolution of the typical plume width along the mean flow direction. The ensemble quantities incorporate an artificial dispersion effect due to lateral center of mass fluctuations of the heat plume from realization to realization. This uncertainty of the lateral plume position is encountered at any point along the mean flow direction. By analogy with the temporal evolution of the dispersion coefficients in heterogeneous media (e.g. [29]) it can be expected that this difference decreases with distance from the injection point. Note that the uncertainty decreases as the temperature samples an increasing part of the medium heterogeneity.

4. Numerical model

The study of heat dispersion is carried out on a three-dimensional heterogeneous aquifer. The source of heat is a GHE at prescribed temperature. The resulting plume is characterized using the stochastic methodology described above.

4.1. Steady state GHE 3D model

The steady state plume created by the GHE is modeled in a $1000 \times 500 \times 500$ m rectangular parallelepiped domain (Fig. 1). Water at a reference temperature T_0 enters the system by the $x = -80$ m plane where flow is prescribed and leaves the domain by the $x = 920$ m side where head is prescribed. The other boundaries are considered impervious. Water is heated by a GHE modeled as a line-like source located at the origin of the coordinate system and extended all along the vertical. The GHE is considered to be at a constant temperature $T_0 + \Delta T$ above the incoming water.

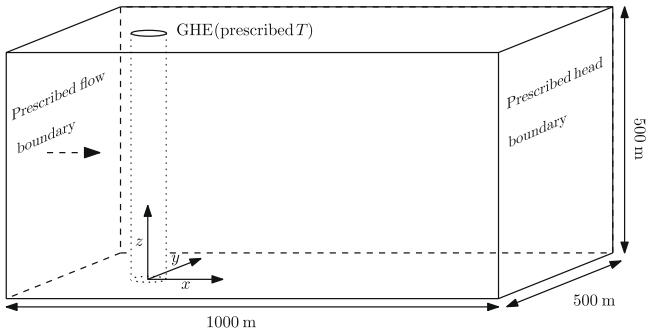

Fig. 1. Groundwater heat exchanger 3D numerical model setup.

All the domain boundaries are adiabatic except the sides where flow and head are prescribed in which the corresponding energy flow is computed. Therefore, the boundary conditions are written as

$$h|_b = H \quad \text{at the outflow,} \tag{18}$$

$$-(K\nabla h)|_b \cdot \mathbf{n} = \begin{cases} q_0 & \text{at the inflow,} \\ 0 & \text{elsewhere} \end{cases} \tag{19}$$

for flow, where H [L] is the value of head prescribed at the outflow, and

$$(-\mathbf{q}T + D\nabla T)|_b \cdot \mathbf{n} = \begin{cases} q_b T_0 & \text{at the inflow,} \\ q_b T & \text{at the outflow,} \\ 0 & \text{elsewhere,} \end{cases} \tag{20}$$

$$T = T_0 + \Delta T \quad \text{at } x, y, z = 0 \tag{21}$$

for transport, where q_b is the flow at the outflow, i.e.,

$$q_b = -(K\nabla h)|_b \cdot \mathbf{n}. \tag{22}$$

Actually, $q_b = q_0$ at the inflow boundary, evenly distributed over the plane, but will be variably distributed over the outflow boundary. These boundary conditions ensure that the mean flow is aligned with the x-direction.

Posed this way, the problem is characterized by the Peclet number Pe

$$Pe = \frac{\rho_w c_w q_0 L}{\lambda}, \tag{23}$$

where L is a characteristic length.

A final comment has to be made on the heat source term. The GHE can be modeled by prescribing either temperature or the dissipated energy. A prescribed temperature boundary condition is preferred here because it allows to compute the influence of heterogeneity in the efficiency of the GHE. However, when temperature is prescribed it is necessary to determine the equivalent radius of the GHE. It should be noticed that, since temperature is only prescribed at one column of nodes, the effective radius depends on grid size and on grid Peclet number. To determine this dependence, heat transport in a bi-dimensional a homogeneous medium was simulated numerically by prescribing T at the GHE. The solution was compared with Eq. (5) for the same dissipated energy. Then the effective radius is given by the isotherm of (5) which corresponds to a temperature perturbation identical to the one imposed in the numerical model in the first place.

Results of the simulations confirmed the dependence with the Peclet number and grid size. For a regular grid of element size $\Delta x = 20$ m, the equivalent radius was between 4 and 4.5 m (approximately $\Delta x/5$) for the range of the Peclet number of this study. This radius was reduced to 2 m by refining the grid around the prescribed temperature zone.

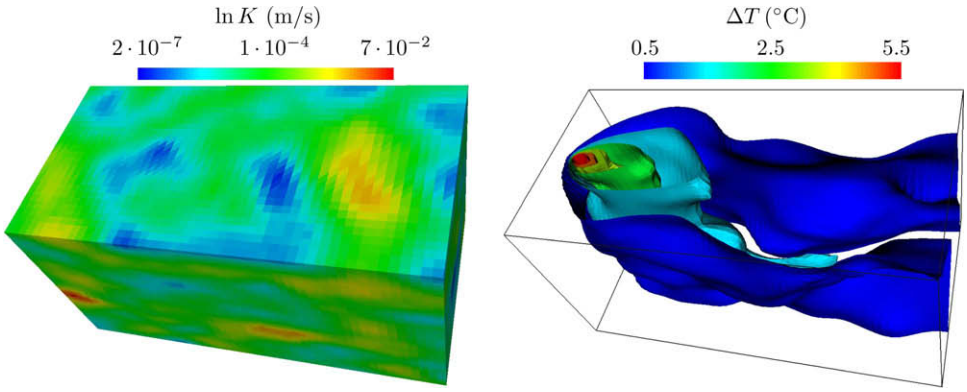

Fig. 2. One realization of the $\ln K$ fields for $\sigma^2_{\ln K} = 3$ (left) and the 0.5, 1.5, 2.5, 3.5 and 5.5 °C isosurfaces of temperature increment above T_0 ($Pe = 14.06$ case) (right).

4.2. Numerical setup

The effect of heterogeneity on heat transport is studied by performing several sets of Monte Carlo simulations. The thermal parameters of the medium are fixed as constant for all simulations: $\lambda = 1.6369$ J/m s K and $\rho_w c_w = 4.18 \times 10^6$ J/m^3 K. The GHE is set 20 °C above reference temperature, i.e., $\Delta T = 20$ °C. The geometric mean of hydraulic conductivity is set to $K_g = 0.392 \times 10^{-4}$ m/s, with variance for $\ln K$, $\sigma^2_{\ln K} = 1, 2$ and 3. The heterogeneity structure of the $\ln K$ field is simulated by an anisotropic Gaussian semivariogram with correlation lengths $L_x = L_y = 2L_z = 100.14$ m. L_z is taken smaller than L_x and L_y to simulate a more realistic bedding structure. A hundred realizations of every case are simulated. Hydraulic conductivity fields are generated using GCOSIM3D [32]. Head is prescribed to 1 m at the outflow boundary. Four different cases corresponding to $Pe = 7.03, 10.23, 14.06$ and 16.62 are simulated by varying the prescribed flow an the inflow, q_0. Pe is computed using L_x as the characteristic length.

The problem is solved using the code Transdens [33] on a triangular prismatic finite element mesh. Discretization is chosen so that there are at least 10 correlation lengths in x and z directions and five elements per correlation length. This ensures a good sampling of the heterogeneity field. The mesh is refined around the heat source to maintain the GHE effective radius within a reasonable range.

4.3. Numerical calculation of heat plume moments

As discussed in Section 3, effective dispersion is computed from the plume moments. Moments, Eqs. (14) and (15), are obtained by means of numerical integration over the nodes of the finite element mesh using a trapezoidal rule. Dispersion coefficient, defined according to (13), where κ_{yy} is given by (14) and (15) for the effective and ensemble dispersion respectively is computed by a forward finite difference scheme.

4.4. Results

4.4.1. Plume dispersion

The effect of heterogeneity on heat dispersion is displayed in Fig. 2. A comparison between the average temperature distribution of the heterogeneous cases and the homogeneous case (Fig. 3) indicates that there is indeed an increment of the lateral extension of the heat plume. The increase in lateral extent is also reflected in a shortening of the temperature isolines, which become less elongated. The effect is proportional to $\sigma^2_{\ln K}$. That is, heterogeneity indeed affects the temperature distribution.

To quantify the effect of heterogeneity on the plume width, the behavior of the second moment of the heat plume (Fig. 4) is analyzed. It can be seen that the width of the plume grows faster with the distance from the source in the heterogeneous cases, which leads to wider plumes. The influence of the domain boundaries manifests itself in the departure of κ_{yy} from the theoretical value for the homogeneous case. When the Peclet number is low, i.e., low water flux, the boundary affects the results at relatively short distances.

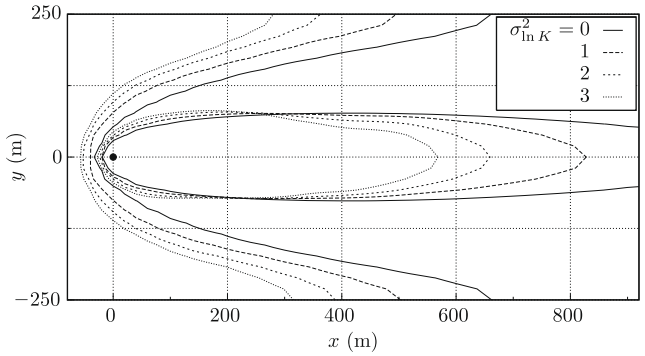

Fig. 3. Comparison between the ensemble temperature for $\ln K$ fields with different $\sigma^2_{\ln K}$ and the homogeneous case ($Pe = 14.06$). Figure shows a section at $z = 250$ m. Isolines correspond to $T_0 + 1$ °C and $T_0 + 0.1$ °C.

Fig. 5 shows the ratio between the heterogeneous and homogeneous transverse dispersion coefficients for the different simulated cases computed using the ensemble and effective second moments (17) and (16). The behaviors of D_T^{ens} and D_T^{eff} reflect the influence of the boundaries on the simulations. The heterogeneous cases display high transverse dispersion near the heat source. The dispersion obtained by the ensemble and the effective second moments are quite similar. Still, as expected, the ensemble dispersion is always higher than the effective one because it quantifies some artificial spreading due to center of mass fluctuations of the plume along the principal flow direction.

The transverse dispersion coefficient also depends on the Peclet number. In the homogeneous media, dispersion is high while diffusion is the dominant process (small Peclet numbers). Dispersion in the heterogeneous media is greater than in the homogeneous one as expected.

An appropriate effective transverse dispersion can be estimated from the deviation of the heterogeneous model results from the homogeneous case. The average dispersion coefficients D_T defined by (17) and (16) can be decomposed into a contribution due to spatial heterogeneity and one due to thermal conductivity as follows:

$$D_T = \alpha_T q_0 + \frac{\lambda}{\rho_w c_w}, \tag{24}$$

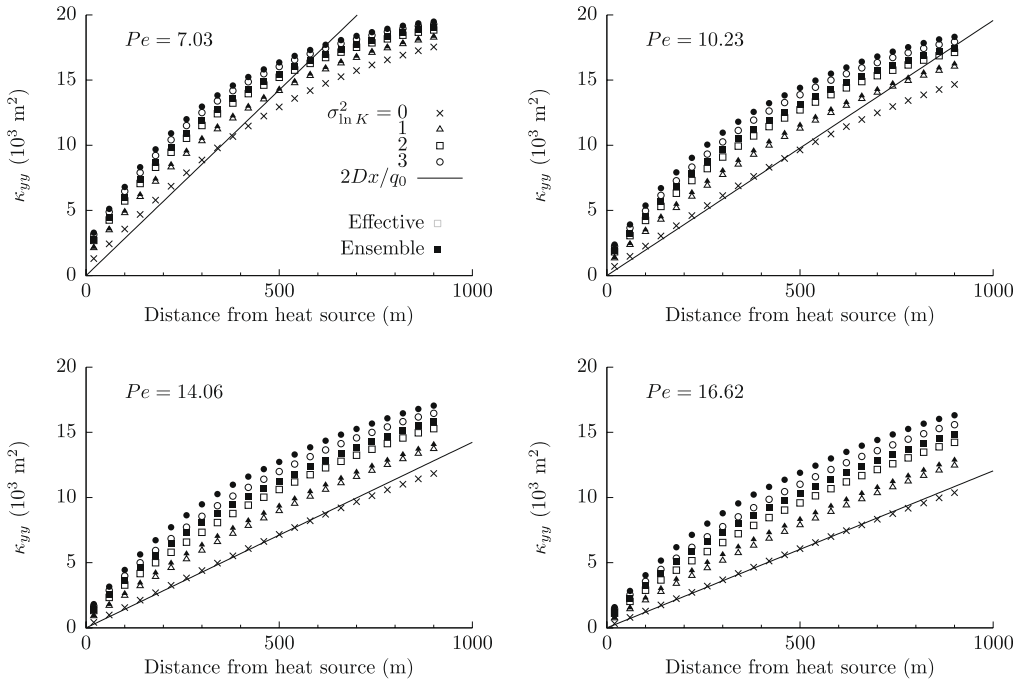

Fig. 4. Effective and ensemble plume second moments for the different values of the Peclet number and $\sigma^2_{\ln K}$. The departure of κ_{yy} for the $\sigma^2_{\ln K} = 0$ case from the theoretical value (solid line) indicates where the boundary effects become relevant.

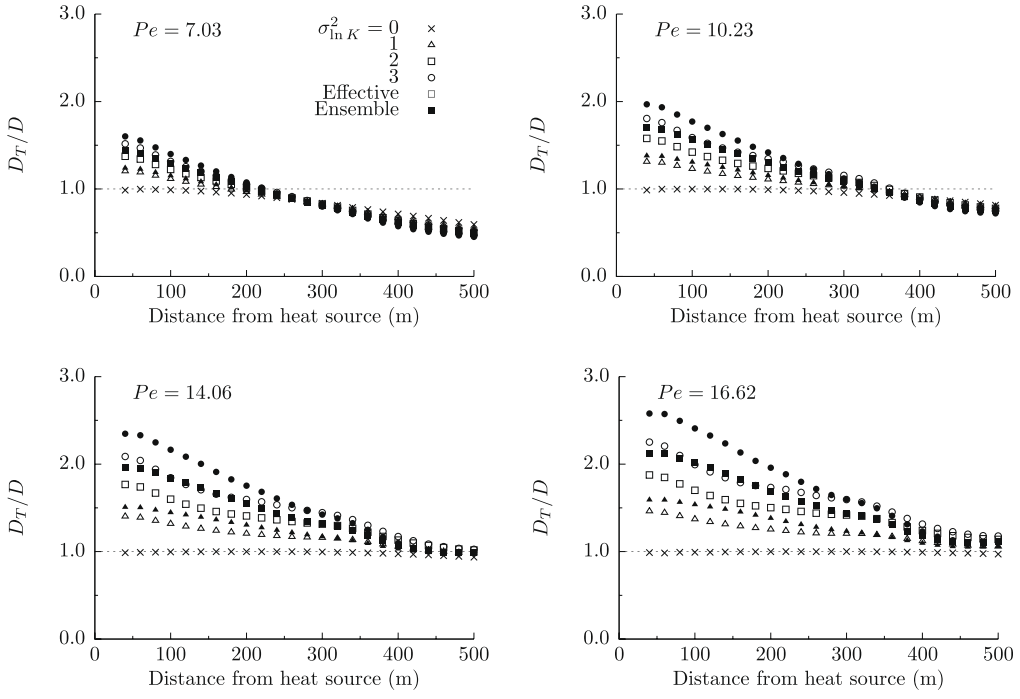

Fig. 5. Ratio between the effective and ensemble transverse dispersion coefficients and the homogeneous dispersion coefficient for different values of the Peclet number and $\sigma^2_{\ln K}$. The horizontal line ($D_T/D = 1$) is the homogeneous case. The departure of the $\sigma^2_{\ln K} = 0$ case from this line indicates where the boundary effects become relevant.

where α_T [L] is the transverse dispersivity. α_T is assumed to be proportional to $\sigma^2_{\ln K}$ and to the correlation length L_x [34], i.e.,

$$\alpha_T = a_T \sigma^2_{\ln K} L_x, \tag{25}$$

where a_T is a dimensionless coefficient dependent on the distance from the source. Using (25) in (24) leads to

$$\frac{1}{\sigma^2_{\ln K}}\left(\frac{D_T}{D} - 1\right) = a_T Pe. \tag{26}$$

The proportionality coefficient a_T at a certain distance from the source can be obtained from a linear fit between the deviation from the homogeneous case and *Pe*. Fig. 6 (left) shows an example of that

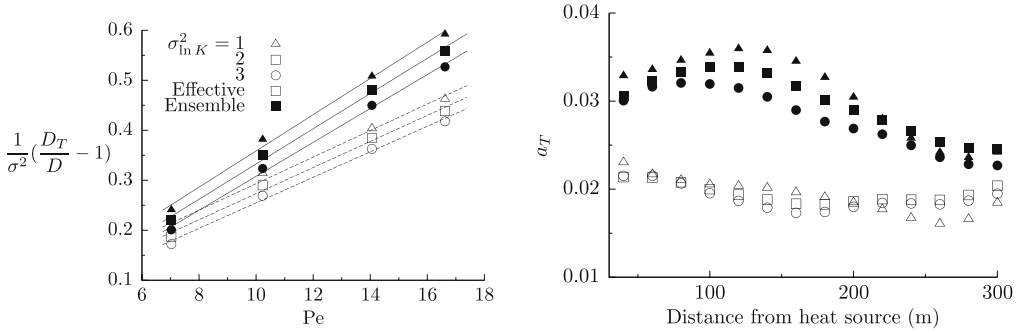

Fig. 6. Left: Dependence of the deviation of D_T from the homogeneous case on the Peclet number (40 m from the heat source). The slope of the fitted line is proportional to transverse dispersion. Right: Dependence of transverse dispersion on the distance from the heat source (taking into account only $Pe = 14.06$ and 16.62 to remove the strong influence of boundaries in the small Pe cases).

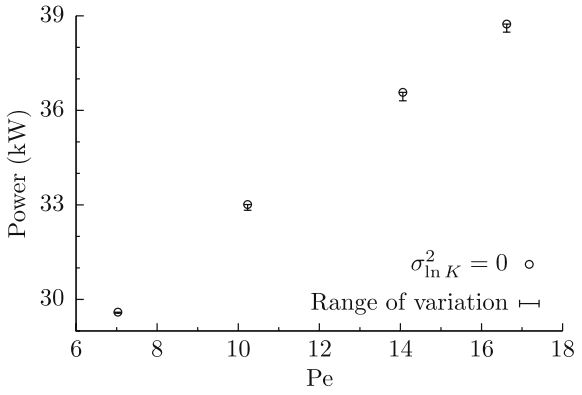

Fig. 7. Dissipated power in the groundwater heat exchanger for the homogeneous case and different Peclet numbers. Bars show the range of average dissipated power for the heterogeneous cases. The lower limit always correspond to the case with highest $\sigma^2_{\ln K}$.

fit for a point at 40 m from the heat source. In order to remove the influence of boundaries in the small Pe cases, only the ones corresponding to $Pe = 14.06$ and 16.62 were taken into account to evaluate a_T. Fig. 6 (right) shows the computed values of a_T for the first 300 m from the heat source. It can be seen that for the ensemble average a_T increases until the first correlation length from the source. Then, it decreases as distance from the source grows. In contrast, for the effective average, a_T displays a less marked dependence on the distance from the source. The difference in the behavior is again caused by the center of mass fluctuations contained in the ensemble magnitudes. For practical purposes, Fig. 6 (right) suggests that the effective transverse dispersion coefficient can be approximated by

$$\alpha_T^{\text{eff}} \approx 0.02\sigma^2_{\ln K} L_x. \tag{27}$$

4.4.2. Energy balance

The above results suggest that heterogeneity may lead to a marked increase in the dissipated energy. However, the GHE dissipated energy for the heterogeneous cases is very similar to that of the homogeneous case (Fig. 7). A very small dependence on $\sigma^2_{\ln K}$ is observed, which is slightly stronger for big Peclet numbers. Therefore, the main controlling factors seem to be the mean flow, i.e., the local flux around the GHE, and the heat conduction, but not dispersion.

5. Conclusions

The role of dispersion in heat transport has been subject to some controversy. The numerical simulations presented in this work show that heterogeneity in the permeability of aquifers causes a dispersive effect on the heat plume generated by a GHE. For the steady state, longitudinal dispersion is negligible and transverse dispersion is proportional to the mean flow q_0, the variance $\sigma^2_{\ln K}$, and correlation length L_x of the log-conductivity field. Ensemble transverse dispersion is high near the heat source (higher than the value for the homogeneous case) and decreases with the distance to the source towards the local dispersion value. However, effective transverse dispersion dependence with the distance from the source is less stronger. Moreover, the amplitude of variation is also smaller. For the conditions simulated here and for modeling purposes $D_T^{\text{eff}} \approx 0.02\sigma^2_{\ln K} L_x q_0$ could be used.

Transverse dispersion determines the shape and width of the heat plume. Therefore, it must be used for models of arrays of GHEs aimed at assessing the impact of thermal groundwater devices. The value of dispersion to be used depends on the objective of the calculations. If the interest is set on the potential spread of the heat signal, which may be the case for environmental impact assessments and risk analysis, then the ensemble dispersion should be used. In that manner, the fluctuations of the center of mass of the plume are taken into account. Thus, the model will provide an estimation of the region that is likely to be affected by the plume. However, if the interest is set on the actual width of the plume and the actual values of temperature, then the effective dispersion should be used.

From the point of view of the efficiency of the GHE, dispersion is not a key factor. The dissipated energy depends solely on the mean flow and on the thermal conductivity. That is, no dispersion should be taken into account when evaluating dissipated energy. This paradox (dispersion needed to assess the temperature plume, but not to compute dissipated energy) may explain the controversy over the use of dispersion. It must be stressed, however, that our finding is restricted to the type of boundary conditions adopted here.

Acknowledgement

This work was performed with funding provided by EU projects FUNMIG (ref. 516514), MUSTANG (ref. 227286) and CICYT project MODEST (ref. CGL2005-05171).

References

[1] Kristmannsdottir H, Armannsson H. Environmental aspects of geothermal energy utilization. Geothermics 2003;32(4–6):451–61.
[2] Ferguson G, Woodbury AD. Thermal sustainability of groundwater-source cooling in Winnipeg Manitoba. Can Geotech J 2005;42(5):1290–301.
[3] Fan R, Jiang Y, Yao Y, Shiming D, Ma Z. A study on the performance of a geothermal heat exchanger under coupled heat conduction and groundwater advection. Energy 2007;32(11):2199–209.
[4] Woodbury AD, Smith L. Simultaneous inversion of hydrogeologic and thermal data. 2. Incorporation of thermal data. Water Resour Res 1988;24(3):356–72.

[5] Nalla G, Shook GM, Mines GL, Bloomfield KK. Parametric sensitivity study of operating and design variables in wellbore heat exchangers. Geothermics 2005;34(3):330–46.
[6] Palmer CD, Blowes DW, Frind EO, Molson JW. Thermal-energy storage in an unconfined aquifer. 1. Field injection experiment. Water Resour Res 1992;28(10):2845–56.
[7] Gehlin SEA, Hellstrom G, Nordell B. The influence of the thermosiphon effect on the thermal response test. Renew Energy 2003;28(14):2239–54.
[8] Fujii H, Itoi R, Fujii J, Uchida Y. Optimizing the design of large-scale ground-coupled heat pump systems using groundwater and heat transport modeling. Geothermics 2005;34(3):347–64.
[9] Nield DA, Bejan A. Convection in porous media. New York: Springer-Verlag; 1992.
[10] Dagan G. Flow and transport in porous formations. New York: Springer-Verlag; 1989.
[11] Gelhar LW. Stochastic subsurface hydrology. Prentice Hall; 1993.
[12] Ferguson G. Heterogeneity and thermal modeling of ground water. Ground Water 2007;45(4):485–90.
[13] Smith L, Chapman DS. On the thermal effects of groundwater-flow. 1. Regional scale systems. J Geophys Res 1983;88(NB1):593–608.
[14] Uffink GJM. Dampening of fluctuations in groundwater temperature by heat exchange between the aquifer and the adjacent layers. J Hydrol 1983;60(1–4):311–28.
[15] Woodbury AD, Smith L. On the thermal effects of 3-dimensional groundwater-flow. J Geophys Res Solid Earth Planets 1985;90(NB1):759–67.
[16] Bear J, Corapcioglu MY. A mathematical-model for consolidation in a thermoelastic aquifer due to hot water injection or pumping. Water Resour Res 1981;17(3):723–36.
[17] Doughty C, Hellstrom G, Tsang CF, Claesson J. A dimensionless parameter approach to the thermal-behavior of an aquifer thermal-energy storage-system. Water Resour Res 1982;18(3):571–87.
[18] Sauty JP, Gringarten AC, Fabris H, Thiery D, Menjoz A, Landel PA. Sensible energy-storage in aquifers. 2. Field experiments and comparison with theoretical results. Water Resour Res 1982;18(2):253–65.
[19] Willemsen A, Groeneveld G. Environmental impacts of aquifer thermal energy storage (ATES): modelling of the transport of energy and contaminants from the store. In: Jousma G, editor. Ground water contamination: use of models in decision-making. Kluwer Academic; 1989. p. 337–51.
[20] Chevalier S, Banton O. Modelling of heat transfer with the random walk method. Part 1. Application to thermal energy storage in porous aquifers. J Hydrol 1999;222(1–4):129–39.
[21] Anderson MP. Heat as a ground water tracer. Ground Water 2005;43(6):951–68.
[22] Gerdes ML, Baumgartner LP, Person M. Convective fluid flow through heterogeneous country rocks during contact metamorphism. J Geophys Res Solid Earth 1998;103(B10):23983–4003.
[23] Porras EA, Tanaka T, Fujii H, Itoi R. Numerical modeling of the Momotombo geothermal system Nicaragua. Geothermics 2007;36(4):304–29.
[24] Diao N, Li Q, Fang Z. Heat transfer in ground heat exchangers with groundwater advection. Int J Therm Sci 2004;43(12):1203–11.
[25] Carslaw HS, Jaeger JC. Conduction of heat in solids. 2nd ed. Oxford: Oxford University Press; 1959.
[26] Aris R. On the dispersion of a solute in a fluid flowing through a tube. Proc Roy Soc London Ser A – Math Phys Sci 1956;235(1200):67–77.
[27] Kitanidis PK. Prediction by the method of moments of transport in a heterogeneous formation. J Hydrol 1988;102(1–4):453–73.
[28] Attinger S, Dentz M, Kinzelbach H, Kinzelbach W. Temporal behavior of a solute cloud in a chemically heterogenous porous medium. J Fluid Mech 1999;386:77–104.
[29] Dentz M, Kinzelbach H, Attinger S, Kinzelbach W. Temporal behavior of a solute cloud in a heterogeneous porous medium. 1. Point-like injection. Water Resour Res 2000;36(12):3591–604.
[30] Fiori A. The relative dispersion and mixing of passive solutes in transport in geologic media. Transp Porous Media 2001;42:69–83.
[31] Dentz M, Carrera J. Effective solute transport in temporally fluctuating flow through heterogenous media. Water Resour Res 2005;41:W08414.
[32] Gomez-Hernandez J, Journel A. Joint sequential simulation of multigaussian fields. In: Soares, editor. Geostat Troia 1992, vol. 1. Kluwer Publ.; 1993. p. 85–94.
[33] Hidalgo JJ, Slooten LJ, Medina A, Carrera J. A Newton–Raphson based code for seawater intrusion modelling and parameter estimation. In: Araguás L, Custodio E, Manzano M, editors, Groundwater and saline intrusion: selected papers from the 18th salt water intrusion meeting. 18th SWIM, Cartagena 2004, no. 15 in Hidrogeología y Aguas Subterraneas, IGME, Madrid; 2005. p. 111–20.
[34] Gelhar LW, Axness CL. Three-dimensional stochastic-analysis of macrodispersion in aquifers. Water Resour Res 1983;19(1):161–80.